

Theory of Oscillating Bodies and its Utilization for Determination of High-temperature Viscosities

D. DUMAS,* K. GRJOTHEIM, B. HÖGDAHL** and H. A. ØYE

*Institute of Inorganic Chemistry, The Technical University of Norway,
N-7034 Trondheim-NTH, Norway*

The theory of the damping of oscillating bodies has been discussed in relation to the determination of viscosities in molten salts. Two approximated equations for the determination of viscosity from the damping of an oscillating cylinder have been derived. An oscillation viscosimeter for measurement of the viscosity of low viscous hygroscopic melts up to 1000°C is described. The viscosities for the following pure molten salts have been determined with an oscillating sphere: MgCl₂: 1.790 cP at 800°C, NaCl: 0.975 cP at 810°C, KCl: 0.975 cP at 800°C. The results for NaCl were found to be in severe disagreement with previously accepted literature values.

The work reported in this paper forms part of a general study on the physico-chemical properties of molten electrolytes used in the electrowinning of light metals. The electrolytes of principal interest for these processes are the alkali-alkaline earth chlorides and the aluminium oxide-alkali cryolite systems. The object of the present work was to develop a satisfactory method for measuring viscosities of low-viscous hygroscopic melts up to 1000°C.

Several methods have been used for the measurement of viscosities at high temperatures.¹⁻⁶ The principles underlying the most frequently used

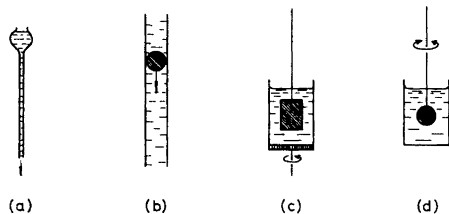


Fig. 1. Methods for determination of viscosity. a) Flow through capillary tube. b) Falling body. c) Rotation with constant velocity. d) Torsional pendulum.

* NATO fellowship. Laboratoire d'Electrochimie et de Physique du Corps Solide, Strasbourg, France.

** Presently at: Mosjøen Aluminiumverk, Elektrokemisk Aluminium A/S, N-8650 Mosjøen, Norway.

methods are shown in Fig. 1. MacKenzie¹ showed that methods (b) and (c) were not suitable for viscosity measurements below 0.1 poise although the last method was used by Bockris and Lowe⁷ down to 0.05 poise. Since the viscosities of interest were around 0.01 poise, serious consideration was given to only two methods, which are referred to in Fig. 1. These are a) the capillary tube method and d) the oscillating body method, which is also called the torsional pendulum method (the pendulum can be either a sphere, cylinder, or a disk).

Both of these methods have been used for the investigation of low viscous fused salts and metals up to 1250°C.¹ Several factors precluded the use of the capillary tube method. These were the difficulty in finding a suitable material for the construction of the capillary and the alteration in the capillary diameter resulting from slight etching and recrystallization. Additional difficulties were encountered in the maintenance of a long zone of constant temperature in the furnace and the visualization of the flow in the capillary. From these considerations it would appear that the oscillating body method is the most suitable. The oscillating body is commonly a sphere and a mathematical relationship between damping and viscosity for this has been well established by Verschaffelt.⁸ Slight changes in the oscillating body must, however, be expected as a result of recrystallization or from chemical attack due to the presence of small amounts of moisture. For this reason the experimental apparatus was designed to use a cylinder as well as a sphere because the cylinder would be simpler to remachine.

In the following sections we review the final relation for an oscillating sphere and develop approximate formulas for the relation between viscosity and damping of a cylinder. Then we present a sketch of the apparatus and give the results of our preliminary studies.

THEORY

Oscillating sphere. A thorough theoretical treatment of a sphere oscillating freely in a viscous liquid has been published in a series of articles by Verschaffelt⁸ in the years 1915–1919.

Verschaffelt assumed the movement of the liquid to be that of concentric, rigid spherical shells performing damped, simple harmonic oscillations around a common z -axis. The liquid was also assumed to exhibit pure Newtonian behaviour. For small oscillations of the sphere, Verschaffelt gave the following differential equation for the motion of the rigid spherical shells:

$$\frac{\partial^2 \omega}{\partial r^2} + \frac{4}{r} \frac{\partial \omega}{\partial r} - \frac{\rho}{\eta} \frac{\partial \omega}{\partial t} = 0 \quad (1)$$

and derived the eqn. (2) which gives viscosity as a function of measurable quantities:

$$\eta = \frac{3\delta I}{4\pi R^3 T_0} \left(\frac{1}{2 + Rb_1 + P} \right)$$

$$P = \frac{b_1 R + 1}{(b_1 R + 1)^2 + b_1^2 R^2} \quad (2)$$

$$b_1 = \sqrt{\frac{\rho\pi}{\eta T}}$$

The symbols are:

- η : viscosity of liquid, poise
- ρ : density of liquid, g cm^{-3}
- R : radius of sphere, cm
- I : moment of inertia of pendulum, g cm^2
- T : time of swing in the liquid, s
- T_0 : time of swing in vacuum (air), s
- δ : logarithmic decrement of the oscillation (defined as the logarithm of the ratio of two successive amplitudes of oscillation).

In eqn. (2) δ represents the friction of the sphere only, and measured values of δ must be corrected for friction against the other parts of the pendulum. In deriving eqn. (2), δ is also assumed to be small, *i.e.* $\delta \ll 2\pi$.

Eqn. (2) must be solved by trial and error and this is most conveniently done by a computer iteration.

Oscillating cylinder. No theoretical treatment of a freely oscillating cylinder has been found in the literature except for the case of a cylinder having infinite length.⁹ It seems difficult to derive a general expression which would give a true picture of the motion of the liquid, since the motion of the liquid near the sharp edges of the cylinder cannot be easily calculated. But we can try

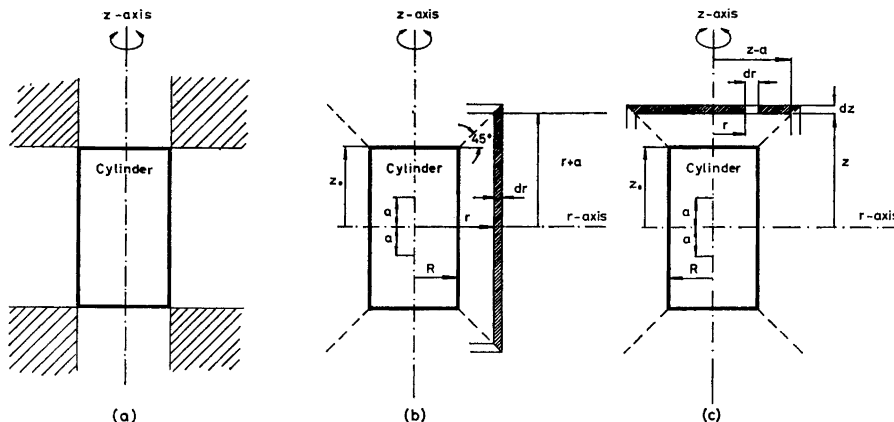


Fig. 2. Cross section of the cylinder and motion of the liquid outside the cylinder surface. a) Part of the liquid unbound to the surface of the cylinder. b), c) Notation for developing the differential equation for the motion of the liquid: b) vertical shell. c) horizontal disk.

to find a model which is possible to treat mathematically and which is not so far from the real picture, despite the fact that the main hypothesis of rigid shells may not necessarily be true. We did this by dividing the motion of the liquid: (i) into vertical cylindrical shells coaxial with the axis of oscillation, and (ii) horizontal discs normal to the axis of oscillation. We also assumed that both, the shells and the discs, were rigid and performed simple harmonic oscillations with the same period and damping as the cylinder. We have chosen to depict the movement of the shells about the cylinder in the following way: a) The cylindrical rings which are shown shaded in Fig. 2a are divided in two different volumes by cones which form an angle of 135° with the cylinder surface. The movement of the shells and discs are extended to the dividing surface. This does not take into consideration the decrease in movement in this area near the edge. b) The motion of the two rings is ignored.

For the frictional force the case a) represents an overcompensation and gives a too low viscosity for the liquid, and the case b) represents an undercompensation giving a too high viscosity value.

Liquid motion at the vertical surface of the cylinder. In Fig. 2 we can see a section of a cylinder with arbitrary height. In the following we define a quantity equal to half of the height (Z_0) minus the radius (R):

$$a = Z_0 - R$$

Analogous to Verschaffelt⁸ we assume the liquid divided in concentric cylindrical shells. Fig. 2b shows a half section of a liquid shell. The distance from the z -axis to the shell is r , the thickness of the shell is dr and half of the height is taken as $r+a$. The oscillation of the shell around the z -axis will give rise to a frictional force per unit area, F_v , on the inner surface. On the outer surface the frictional force, opposite in sign, will be:

$$- \left(F_v + \frac{\partial F_v}{\partial r} dr \right)$$

If we now assume the shell to rotate a small angle α in unit time: $\partial\alpha/\partial t$, we can equate the work done on the shell by the frictional force to the increase in kinetic energy of the same shell. Remembering that $r(\partial\alpha/\partial t) = r\omega$ gives the linear velocity we obtain with reference to Fig. 2b.:

$$\begin{aligned} F_v [2\pi r \cdot 2(r+a)] r \frac{\partial\alpha}{\partial t} - \left[F_v + \frac{\partial F_v}{\partial r} dr \right] [2\pi(r+dr)2(r+a+dr)(r+dr)] \frac{\partial\alpha}{\partial t} \\ = \frac{\partial}{\partial t} (\frac{1}{2}mv^2) = 2\pi r dr \cdot 2(r+a+dr) \rho r \frac{\partial\alpha}{\partial t} r \frac{\partial\omega}{\partial t} \end{aligned} \quad (3a)$$

After reduction and collecting only first order terms with respect to dr we obtain:

$$-[2(r+a)+r]F_v - r(r+a) \frac{\partial F_v}{\partial r} = r^2(r+a) \frac{\partial\omega}{\partial t} \quad (3b)$$

The liquid is assumed to be pure Newtonian, so that:

$$F_v = -\eta r \frac{\partial\omega}{\partial r} \quad (4)$$

where η is the viscosity of the liquid. The combination of eqn. (3b) and (4) gives:

$$\frac{\partial^2 \omega}{\partial r^2} + \left(\frac{3}{r} + \frac{1}{r+a} \right) \frac{\partial \omega}{\partial r} - \frac{\rho}{\eta} \frac{\partial \omega}{\partial t} = 0 \quad (5)$$

The solution of this general equation will result in complex hypergeometric functions. We can make the treatment simpler in the following case:

$a=0$, cylinder with the height equal to the diameter. Implicit in this model is that the liquid moves as vertical rigid shells extending up and down to the angle 135° from the edges of the cylinder.

$a \rightarrow \infty$, cylinder of infinite height. Here the differential equation we find agree with the picture where the motion of the two rings are ignored whatever the height of the cylinder may be.

First case: $a=0$. Eqn. (5) reduces to eqn. (6):

$$\frac{\partial^2 \omega}{\partial r^2} + \frac{4}{r} \frac{\partial \omega}{\partial r} - \frac{\rho}{\eta} \frac{\partial \omega}{\partial t} = 0 \quad (6)$$

This is the same equation as that Verschaffelt obtained for the sphere. Referring to his work⁸ the general motion of a damped harmonic oscillation is given by the general expression:

$$\alpha_r = \phi(r) e^{-\delta t/T} \cos \left(\frac{2\pi}{T} t - \psi(r) \right) \quad (7)$$

The symbols are

α_r = angular amplitude of oscillations

t = time

r = distance from the axis of rotation

T = time of swing

δ = logarithmic decrement or damping constant defined by

$$\delta = \ln[\alpha(t)/\alpha(t+T)]$$

Here $\phi(r)$ and $\psi(r)$ are functions of r only and determine how the amplitude and phase are changed by increasing the distance r from the axis.

The motion described by eqn. (6) will in fact give a wave motion propagating out in the liquid. The amplitude of the wave is steadily damped down by the friction due to viscosity of the liquid. Instead of using the form of eqn. (7) it is more convenient to introduce complex functions and it is well known that eqn. (7) can be considered the real part of

$$\alpha_r = u(r) e^{kt} \quad (8)$$

where $u(r)$ is a complex function of r and k is a complex constant. In accordance with the former assumptions for the motion we have the equation for the cylinder similar to eqn. (8):

$$\alpha = A e^{kt} \quad (9)$$

Setting

$$\begin{aligned} u &= u_1 + iu_2 \\ k &= k_1 + ik_2 \end{aligned} \quad (10)$$

and introducing trigonometric functions and comparing with eqn. (7) we obtain:

$$k_1 = -\delta/T \text{ and } k_2 = 2\pi/T \quad (11)$$

This equation relates k to δ and T which both can be determined experimentally.

For the determination of u we first note that from eqn. (8) we get

$$\frac{\partial \alpha_r}{\partial t} = \omega = ku e^{kt} \quad (12)$$

Inserting eqn. (12) in eqn. (6):

$$\frac{d^2u}{dr^2} + \frac{4}{r} \frac{du}{dr} - b^2u = 0 \quad (13)$$

with

$$b = \sqrt{\rho k / \eta}$$

Expressing b as a function of the complex quantity from eqn. (10):

$$b = \sqrt{(\rho/\eta T)(2\pi i - \delta)} \quad (14a)$$

If δ is small relative to 2π , we can neglect it in the above expression and get:

$$b = \sqrt{\pi \rho / \eta T} (1+i) = \sqrt{2\pi \rho / \eta T} e^{i\pi/4} = b_0 e^{i\pi/4} \quad (14b)$$

$$b_0 = \sqrt{\frac{2\pi \rho}{\eta T}}$$

The solution to eqn. (13) is found to be

$$u = A \frac{R^3}{r^3} \frac{br+1}{bR+1} e^{-b(r-R)} \quad (15a)$$

and the solution of eqn. (6), the real part of eqn. (15b):

$$\omega = kA \frac{R^3}{r^3} \frac{br+1}{bR+1} e^{-b(r-R) + kt} \quad (15b)$$

As the boundary conditions we have used

1. $u = u(R) = A$ for $r = R$
2. $u = 0$ for $r \rightarrow \infty$

The A in eqn. (15) is the same as in eqn. (9) and hence the first boundary condition implies the well established assumption that the liquid perfectly wets the cylinder. The second boundary condition is of course pure analytical. However, as shown by Verschaffelt⁸ for a sphere, in the liquid the damping of the wave propagating outwards is so pronounced that for all practical purposes condition 2 above can be used if

$$\exp[-2b(R_1 - R)] \ll 1$$

where R is the radius of the sphere and R_1 , the radius of the vessel holding the liquid. In our later experiments with a sphere we have

$$\exp[-2b(R_1 - R)] \simeq 10^{-4} \ll 1$$

justifying the use of the second boundary condition above. We assume this condition to be fulfilled for the case of a cylinder also.

Second case: $a \rightarrow \infty$. The differential equation (5) reduces to:

$$\frac{\partial^2 \omega}{\partial r^2} + \frac{3}{r} \frac{\partial \omega}{\partial r} - \frac{\rho}{\eta} \frac{\partial \omega}{\partial t} = 0 \quad (16)$$

We now again try the solution of eqn. (12) and by insertion in eqn. (16) we find:

$$\frac{d^2 u}{dr^2} + \frac{3}{r} \frac{du}{dr} - b^2 u = 0 \quad (17)$$

This equation can be compared with eqn. (13) in the first derivation. The only difference is the factor 3 instead of 4 but eqn. (21) is much more difficult to solve because the coefficient of $(1/r)(du/dr)$ is not even. The details in the solution procedure is omitted but it can be shown that the solution of eqn. (17) are Bessel functions. It is possible to rewrite the equation using Kelvin functions:

$$u(r) = \left(A \frac{R}{r} \right) \frac{\ker_0(b_0 r) + i \cdot \text{kei}_0(b_0 r)}{\ker_1(b_0 R) + i \cdot \text{kei}_1(b_0 R)} \quad (18a)$$

The solution of eqn. (16) will be, the real part of eqn. (18b)

$$\omega = k \left(A \frac{R}{r} \right) \frac{\ker_0(b_0 r) + i \cdot \text{kei}_0(b_0 r)}{\ker_1(b_0 R) + i \cdot \text{kei}_1(b_0 R)} e^{kt} \quad (18b)$$

Liquid motion at the horizontal surface of the cylinder. By reference to Fig. 2c we can derive a corresponding expression for the horizontal sections. If we choose a disc, having a thickness denoted by dz there exists on the underside a frictional force per unit area F_h and on the upper side a frictional force opposite in sign:

$$-\left(F_h + \frac{\partial F_h}{\partial z} dz \right)$$

Again we assume the disc to rotate around the z -axis at a small angle $\partial\alpha/\partial t$ and we can then equate the work done by the frictional forces on the disc to the increase in kinetic energy of the same disc. Since the linear velocity of the disc changes with the distance r from the z -axis, we must perform an integration over the disc. Noting that in this integration z and dz are constants we get:

$$\begin{aligned} & \int_0^{(z-a)} F_h r \frac{\partial \alpha}{\partial t} 2\pi r \, dr - \int_0^{(z-a)+dz} \left(F_h + \frac{\partial F_h}{\partial z} dz \right) r \frac{\partial \alpha}{\partial t} 2\pi r \, dr \\ &= \int_0^{(z-a)+dz/2} \frac{\partial}{\partial t} \left(\frac{1}{2} m V^2 \right) 2\pi r \, dr = \int_0^{(z-a)-dz/2} \rho dz r \frac{\partial \alpha}{\partial t} r \frac{\partial \omega}{\partial t} 2\pi r \, dr \end{aligned} \quad (19)$$

The frictional force can be expressed by Newtons viscosity law:

$$F_h = -\eta r \frac{\partial \omega}{\partial z} \quad (20)$$

Inserting F_h and $\partial F_h / \partial z$ in eqn. (19) and integrating eqn. (19) we finally get after collecting only first order terms:

$$\frac{\partial^2 \omega}{\partial z^2} + \frac{4}{z-a} \frac{\partial \omega}{\partial z} - \frac{\rho}{\eta} \frac{\partial \omega}{\partial t} = 0 \quad (21)$$

Now, we can treat the same cases as previously:

First case: $a=0$. We find the equation corresponding to eqn. (15b):

$$\omega = kA \frac{Z_0^3}{z^3} \frac{bz+1}{bZ_0+1} e^{-b(z-Z_0)+kt} \quad (22)$$

As R_0 is equal to Z_0 in this case eqn. (15) and eqn. (22) becomes identical which means that the sections can be connected at the line 135° out from the edges of the cylinder giving rise to no extra disturbances at the connecting boundaries.

Second case: $a \rightarrow \infty$. Eqn. (21) reduces to the following equation:

$$\frac{\partial^2 \omega}{\partial z^2} - \frac{\rho}{\eta} \frac{\partial \omega}{\partial t} = 0 \quad (23)$$

which is simple to resolve by introducing u as before and using the same boundary conditions:

$$\omega = kA e^{-b(z-Z_0)+kt} \quad (24)$$

Moment of the frictional forces. Now we intend to show that it is possible to write the moment of the frictional forces on the cylinder in the following form:

$$C = L(d\alpha/dt) \quad (25)$$

L being a constant.

First case: $a=0$. The moment on the vertical surface:

$$C_v = RF_v 2\pi R 2Z_0 \quad (26a)$$

Referring to eqn. (4):

$$C_v = -4\pi R^2 Z_0 \eta (\partial \omega / \partial r)_R \quad (26b)$$

Inserting eqn. (15b):

$$C_v = 4\pi R^2 Z_0 \eta \frac{b^2 R^2 + 3bR + 3}{bR + 1} \frac{d\alpha}{dt} \quad (26c)$$

For the horizontal sections:

$$C_h = 2 \int_0^R r F_h 2\pi r dr \quad (27a)$$

Referring to eqn. (20) we find after integration:

$$C_h = -\pi R^4 \eta (\partial \omega / \partial z)_{Z_0} \quad (27b)$$

Inserting eqn. (22):

$$C_h = \pi R^4 \eta \frac{b^2 Z_0^2 + 3bZ_0 + 3}{Z_0(bZ_0 + 1)} \frac{d\alpha}{dt} \quad (27c)$$

Adding eqns. (26c) and (27c), setting $Z_0=R$, we find an equation of which the real part represents the moment of the frictional forces corresponding to a cylinder with the height equal to the diameter, according to Fig. 3a.

$$C = C_v + C_h = 5\pi R^3 \eta \frac{b^2 R^2 + 3bR + 3}{bR + 1} \frac{d\alpha}{dt} \quad (28)$$

From eqn. (14a) we can get the real part of eqn. (28):

$$\text{Re}(C) = 5\pi R^3 \eta (2 + Rb_1 + P) \frac{d\alpha}{dt} \quad (29)$$

with

$$P = \frac{b_1 R + 1}{(b_1 R + 1)^2 + b_1^2 R^2}, \quad b_1 = \sqrt{\frac{\pi \rho}{\eta T}}$$

Second case: $a \rightarrow \infty$.

By departing from the same eqns. (26b) and (27b) but using eqns. (18b) and (24) to find respectively $(\partial\omega/\partial r)_R$ and $(\partial\omega/\partial z)_Z$, we obtain:

$$C_v' = 4\pi R^3 Z_0 \eta \left[\frac{2}{R} - b_0 e^{3\pi i/4} \frac{\text{ker}_0(b_0 R) + i \cdot \text{kei}_0(b_0 R)}{\text{ker}_1(b_0 R) + i \cdot \text{kei}_1(b_0 R)} \right] \frac{d\alpha}{dt} \quad (30)$$

$$C_h' = \pi R^4 b \eta \frac{d\alpha}{dt} \quad (31)$$

Adding eqns. (30) and (31) and setting $Z_0=R$ we find a relation in the real part which represents the moment of the frictional forces according to Fig. 3b

$$C' = C_h' + C_v' = 4\pi R^4 \eta \left[\frac{b}{4} + \frac{2}{R} - b_0 e^{3\pi i/4} \frac{\text{ker}_0(b_0 R) + i \cdot \text{kei}_0(b_0 R)}{\text{ker}_1(b_0 R) + i \cdot \text{kei}_1(b_0 R)} \right] \frac{d\alpha}{dt} \quad (32)$$

To find the real part of this equation we will transform the last factor using numerical values for Kelvin functions tabulated from MacLachlan,⁹ according to:

$$\text{ker}_\nu(Z) + i \cdot \text{kei}_\nu(Z) = N_\nu(Z) \exp[i\phi_\nu(Z)] \quad (33)$$

where $N_\nu(Z)$ and $\phi_\nu(Z)$ are tabulated. We can then write:

$$\text{Re}(C') = 4\pi R^4 \eta \left(\frac{b_0}{4\sqrt{2}} + \frac{2}{R} - b_0 \frac{N_0(b_0 R)}{N_1(b_0 R)} \cos\left(\frac{3}{4}\pi + \phi_0(b_0 R) - \phi_1(b_0 R)\right) \right) \frac{d\alpha}{dt} \quad (34)$$

Motion of the cylinder. The movement of an oscillating body hanging freely in a torsional wire is given by the wellknown differential equation:

$$I \frac{d^2\alpha}{dt^2} + C + M\alpha = 0 \quad (35)$$

where

α = angular displacement

t = time

I = moment of inertia of the cylinder

M = torsional constant of the wire

C = the sum of the moment of frictional forces on the cylinder surface.

We have seen, in the previous section, that we can write C in the form:

$$C = L(d\alpha/dt) \quad (36)$$

L being independent of t . Eqn. (35) can then be rewritten:

$$I \frac{d^2\alpha}{dt^2} + L \frac{d\alpha}{dt} + M\alpha = 0 \quad (37)$$

By introducing eqn. (9), expressing L as a complex quantity, and introducing the time of swing in vacuum

$$T_0 = 2\pi \sqrt{I/M}$$

it is possible to relate the real part of L to measurable quantities:

$$\text{Re}(L) = \frac{I\delta}{T} \left(\frac{T^2}{T_0^2} \frac{4\pi^2}{4\pi^2 + \delta^2} + 1 \right) \quad (38)$$

In our system, we can write with an error less than 0.01 %

$$T = T_0$$

and we can neglect δ^2 when compared to $4\pi^2$, with an error less than 0.004 %.

We hence get:

$$\text{Re}(L) = \frac{2I\delta}{T_0} \quad (39)$$

Viscosity equation for the cylinder. We have previously expressed the moment of frictional forces in terms of the viscosity and measurable quantities and by combining these equations with eqns. (39) and (36) we are now able to relate the viscosity to measurable quantities for the two models of liquid motion.

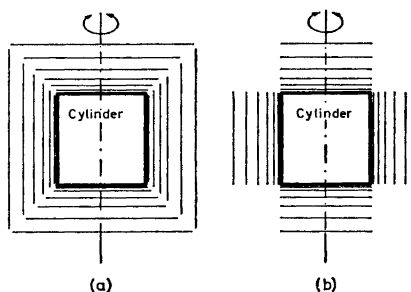


Fig. 3. Illustration of the two idealized pictures of the liquid motion, concerning a cylinder the length of which is equal to the diameter: a) Eqn. (35); b) Eqn. (36).

Model a): Motion as depicted on Fig. 3a. The shells and discs are supposed to be rigid performing harmonic oscillations. By combination of eqns. (39), (36) and (29) is obtained

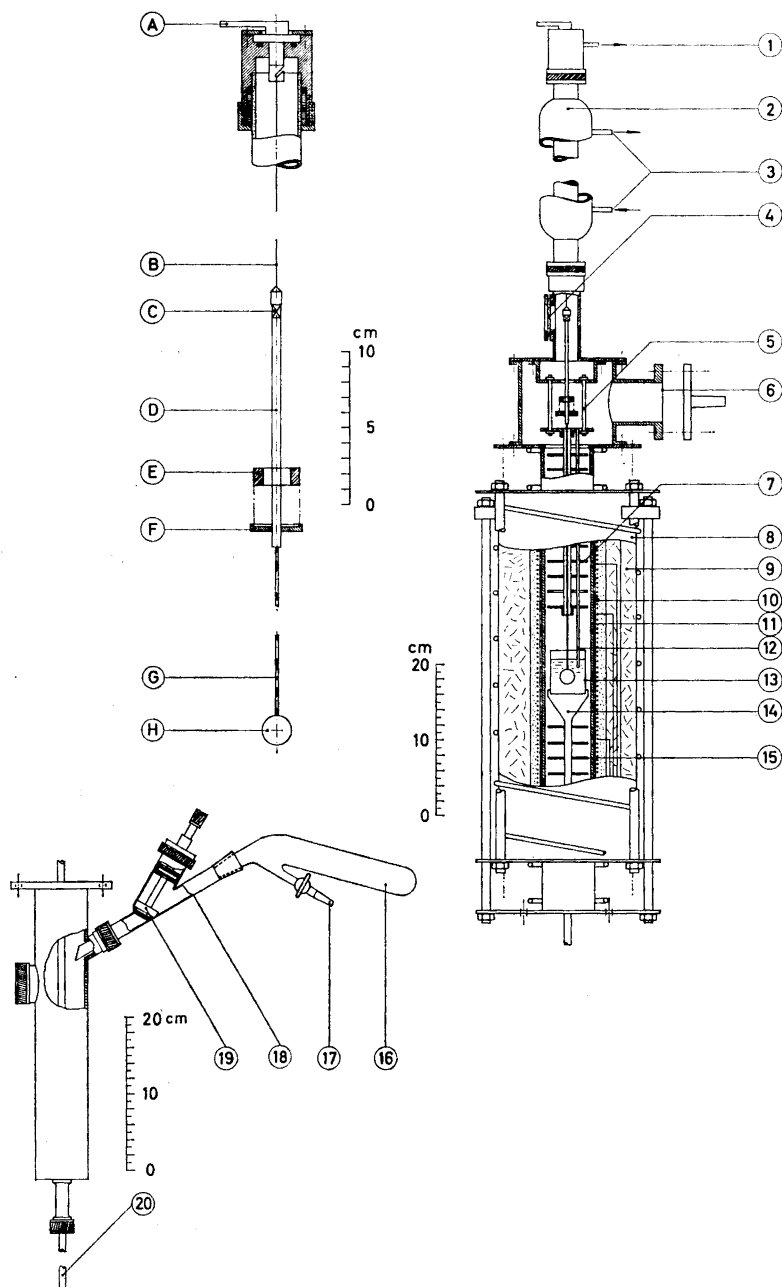


Fig. 4. Diagram of oscillating pendulum and furnace assembly.
 A: Handle for start oscillations; B: Tungsten torsion wire; C: Mirror; D: Brass rod; E: Ni ring; F: Ni disk; G: Pt-10 % Ir rod; H: Pt-10 % Ir sphere.

$$\eta = \frac{2I\delta}{5\pi R^3 T_0} \frac{1}{2 + Rb_1 + P}$$

$$P = \frac{b_1 R + 1}{(b_1 R + 1)^2 + b_1^2 R^2} \quad (40)$$

$$b_1 = \sqrt{\frac{\pi\rho}{\eta T}}$$

It may be noted that eqn. (40) for this cylinder is actually the same as eqn. (2) for the sphere except for the factor $2/5$ which for the sphere is $3/4$.

Model b). Motions as depicted on Fig. 3b. The shells and rings are supposed to be rigid, performing harmonic oscillations but motion in the liquid not being perpendicular on the cylinder surface is excluded. By combination of eqns. (39), (36) and (34) is obtained:

$$\eta = \frac{2I\delta}{T_0} \frac{1}{A} \quad (41)$$

$$A = 4\pi R^4 \left[\frac{b_0}{4\sqrt{2}} + \frac{2}{R} - b_0 \frac{N_0(b_0 R)}{N_1(b_0 R)} \cos\left(\frac{3}{4}\pi + \phi_0(b_0 R) - \phi_1(b_0 R)\right) \right]$$

$$b_0 = \sqrt{2\pi\rho/\eta T}$$

It should again be noted that the δ to be used in eqn. (41) is due to viscous damping on the cylinder only. The δ obtained from experiments must hence be corrected for damping due to friction on the other parts of the pendulum.

EXPERIMENTAL

Apparatus. In Fig. 4 a sketch is given of the apparatus constructed for our experimental work. The oscillating part is shown separately to the left.

A polished Pt-10 % Ir sphere (H) or cylinder was attached to a 1.5 mm diameter rod (G) of the same material. The diameter of the sphere and cylinder was 20 mm, the height of the cylinder was approximately 20 mm. The platinum rod was screwed tightly into a 6 mm diameter brass rod (D) making a rigid pendulum which was then joined to a tungsten torsion wire (B). A plane mirror (C) mounted near the top of the brass-rod was used for measuring the movement. A disk of pure Ni (F) was attached to the brass-rod. An extra Ni ring (E) can be taken on and off when it is required to determine the moment of inertia of the system. The oscillations were initiated by slightly turning the handle (A) at the extreme top of the apparatus. The tungsten wire was surrounded by a thermostated, double-walled mantle (2) made of pyrex glass. During measurements the temperature was maintained at $25 \pm 0.1^\circ\text{C}$ by circulating water through the mantle (3) from an ordinary thermostatically controlled water bath. The mirror on the pendulum was aligned with a glass window (4) so that the oscillations of the pendulum could be made visible by means of a light beam. This beam came in from the left, passed through the

1: Outlet inert gas; 2: Thermostated mantle; 3: In- and outlet of thermostated water; 4: Glass window; 5: Screws for adjustment of upper radiation shield; 6: Flange for connection to vacuum line; 7: Upper radiation shields; 8: Water-cooled furnace jacket; 9: Diatomaceous earth for insulation; 10: Kanthal heating wire; 11: Pythagoras tube; 12: Pt-10 % Rh thermocouple; 13: Pt crucible; 14: Supporter; 15: Lower radiation shields; 16: Container; 17: Inlet inert gas; 18: Glass system; 19: Valve; 20: Piston.

window and was reflected by the mirror on a scale mounted about 1.5 m to the left of the apparatus. A deflection of 0.04° corresponded to 1 mm on this scale. Calculations have shown that the error due to refraction of the light beam in the window was negligible.

The crucible (13) used was a Pt-crucible of 45 mm I.D. and height 80 mm.

A standard type furnace as described by Motzfeldt¹⁰ was used. It consisted of a central Pythagoras-tube (11) with a heating element (10) of resistance wire (Kanthal A). The element was thermally insulated by diatomaceous earth (9) and enclosed by a water-cooled jacket (8).

The heating element was made by winding resistance wire around the central tube from the base to the top and then reversing the process so that the downward windings lie in between the upward windings. This was done to eliminate magnetic fields inside the furnace which could give rise to disturbances in the melt due to convection or damping resulting from eddy currents in the platinum pendulum. The temperature was regulated and kept constant by connecting a Variac to a voltage-stabilizer. The temperature distribution was adjusted by shunting parts of the windings. A temperature variation of less than $\pm 0.5^\circ\text{C}$ was obtained within the crucible over the time of one viscosity experiment. No disturbance due to convection flows in the melt was observed below 950°C . The temperature was measured by a potentiometer and a Pt/Pt-10 % Rh thermocouple (12) which dipped into the melt.

The upper part of the apparatus together with the thermostated glass mantle which included the glass window was stationary, and was mounted on a rigid rack, while the rest of the apparatus was mounted on a trolley and was able to slide up and down. The upper radiation shields (7) were fixed to the upper stationary part of the apparatus by three screws (5). These screws made it possible to slightly adjust the position of the radiation shields to secure free pendulum swing.

The supporter (14) together with radiation shields (15) could be moved relative to the furnace tube so that the position of the crucible could be adjusted. In addition to this the supporter bearing crucible could be lowered by means of a piston (20) below the point where it was possible to fill it by means of the glass system (18). This system allowed the container (16) to be filled with hygroscopic salt in a dry box and, after closing the valve (19), to transfer it and mount it on the furnace. Before opening the valve the furnace was evacuated. After passing dry nitrogen through the furnace we could transfer the salt from the container to the crucible. The same system was afterwards used to add non-hydroscopic salts.

The whole apparatus was made vacuumtight by rubberseals on all the flanges. Connection to the vacuum system was made by an upper flange (6). With this system we could obtain a vacuum down to 3×10^{-4} torr.

Preparation of pure salts. In our experiments we used NaCl and KCl *p.a.* from Merck, Darmstadt (Germany) and MgCl_2 *p.a.* from J.T. Baker.

Both NaCl and KCl were dried under a primary vacuum (10^{-2} torr) at a temperature of 500 to 600°C . The salts were then melted under a stream of nitrogen and were then allowed to crystallize as the temperature was slowly lowered. Unclear crystals were discarded. MgCl_2 was prepared very carefully by treatment with HCl. We used a method which we have previously described.¹¹ This was a combination of the methods already used by Laitinen *et al.*¹² for LiCl and by Schrier¹³ for MgCl_2 . Analysis by polarographic measurements¹³ did not reveal any detectable amount of water.

Calibration of the apparatus. Eqns. (2), (40) and (41) give the viscosity from the measurement of the damping of a torsional pendulum and the periods of swing in the melt and in the gas. We also need to know the density of the melt as well as the following parameters effecting the system: moment of inertia, radius of the body and damping correction.

The period of a harmonic pendulum in a gas is given by the relation:

$$T_0 = 2\pi\sqrt{I_0/M} \quad (42)$$

with I_0 moment of inertia and M torsional constant of the wire. I_0 cannot be found directly by measurement of the period because we do not know M . But by adding and taking away a mass with known moment of inertia it can be computed, using relation (43).

$$I_0 = \Delta I \frac{T_0^2}{(T_0^2 - T^2)} \quad (43)$$

where T_0 and T are the time of swing with and without the extra mass, respectively, ΔI is the moment of inertia of the extra mass. This determination is quite critical for the accuracy of the viscosity measurements. Calculation shows that a variation of 0.02 % in the period will introduce an error close to 0.15 % in the moment of inertia. The period was extremely sensitive to the handling of the oscillating system. To decrease the effect due to changes in the torsional constant of the wire, it was pretreated at 1200°C in an atmosphere¹⁴ of dry hydrogen. It was also found necessary to allow time for the stabilization of the wire following the removal or addition of the extra mass (E). This is shown in Table 1. The wire had a diameter of 0.2 mm

Table 1. Change in periods by taking off and adding the extra mass.

	Extra mass added	Extra mass taken off	Extra mass added again
Period	5.103 ± 0.001	3.627	5.112
in seconds		↓ one week 3.643 ± 0.001	↓ two days 5.103 ± 0.001

and all measurements were carried out at 25°C. Trials with thinner wires showed instability with respect to torsional constant. The added mass had a moment of inertia of $\Delta I = 92.05 \text{ g}\cdot\text{cm}^2$. The sphere and the cylinder had radii of 1.053 and 1.015 cm, giving a moment of inertia at 25°C of 46.7 and 71.8 $\text{g}\cdot\text{cm}^2$, respectively.

For measurements at elevated temperatures it was necessary to make corrections for the expansion of the sphere or cylinder. The average linear coefficient of expansion between 0 and 1000°C for platinum is 9×10^{-6} ,¹⁵ and since the moment of inertia is proportional to the square of the radius, we obtain for the sphere:

$$I_t = 141.45 + 46.70(1 + 2(t - 25) \times 9 \times 10^{-6})$$

and for the cylinder:

$$I_t = 141.45 + 71.80(1 + 2(t - 25) \times 9 \times 10^{-6})$$

To determine the viscosity we have to consider the damping of the body (sphere or cylinder) due to the viscous drag in the melt. We measure the damping δ_1 of the whole system, and have to correct this value by subtracting the damping for the system outside the crucible. This correction is given by the expression:

$$\delta_2 - \delta_3 \quad (44)$$

where δ_2 = observed damping of the system in nitrogen atmosphere, and δ_3 = calculated damping of the oscillating body only, in nitrogen atmosphere. This expression is expected to be approximately constant since most of the damping will occur in the tungsten wire and on the brass system which are held at constant temperature. Strictly, a correction for the part of the platinum rod submerged in the liquid should be performed, but calculation showed this effect to be negligible.

Observed readings of the amplitude were plotted as ordinate against the number of oscillations as abscissa, noting that the successive readings on each side are phase-shifted by half a wavelength. One then obtains two symmetric exponential curves and finds graphically the zero line midway between the curves. Corrected amplitudes are now obtained as the distance from the zero line to one of the exponential curves. In a new graph the logarithm of this corrected amplitude is plotted *versus* number of oscillations, and straight lines were obtained indicating damped, simple harmonic motions. A check of simple harmonic motion is that the time of swing was independent of the amplitude.

From the slope of the straight line we find the damping constant δ according to the equation:

$$\delta = (\ln \alpha_n - \ln \alpha_{n+k})/k \quad (45)$$

α_n and α_{n+k} are the respective amplitudes at oscillation number n and $n+k$.

The obtained correction term is given in Table 2. This correction can be used independent of the temperature in the furnace.

$$\delta_2 - \delta_3 = 0.00325 \pm 0.00006$$

Computation of the viscosity. For measurements with the sphere, the viscosities were calculated by an electronic computer using an iteration procedure according to eqn. (2).

Table 2. Correction for the damping ($\delta_2 - \delta_3$).

Temperature, °C	$\delta_2 \times 10^3$ measured	$\delta_3 \times 10^3$ computed	$(\delta_2 - \delta_3) \times 10^{-3}$
25	3.33	0.10	3.23
410	3.35	0.16	3.19
700	3.49	0.19	3.30
850	3.49	0.21	3.28

The starting guess of the viscosity is not critical and 0.01 poise has been used for all calculations.

For measurements with the cylinder, viscosities were calculated manually by two iterations and a graphical extrapolation, both according to eqn. (40) and to eqn. (41) and using tabulated Bessel functions in McLachlan.⁹

RESULTS

Viscosity measurements in water and KNO₃. In Table 3, we give results that were obtained (with the sphere) in water and KNO₃, so that a check could be made on our apparatus. Three measurements were made at each temperature. The scattering of our results was less than 1%. For water we used the density data given in Landolt-Börnstein's tables.¹⁶ For KNO₃ we used the following relation

$$d_t = 2.144 - (0.80 \times 10^{-3})t$$

Table 3. Viscosity in water and KNO₃. Corresponding reference according to Landolt-Börnstein¹⁶ for H₂O and Kleinschmidt²⁰ for KNO₃.

Compound	Temperature, °C	Damping, δ	Viscosity, cP	
			This work	Literature data
H ₂ O	15.9	0.01477	1.118	1.114
	18.1	0.01427	1.064	1.068
	19.0	0.01401	1.036	1.030
	20.9	0.01357	0.986	0.983
KNO ₃	342	0.03240	2.700	2.720
	382	0.02726	2.255	2.257
	398	0.02876	2.070	2.085

in the temperature range of 336–400°C, as given by Brillant.¹⁷

The value for water was actually found to be systematically 2 % lower than the literature value. This is believed to be due to difficulties in determination of the radius of the sphere (see below) and a correction factor according to this deviation was used for all experiments. By this calibration good agreement with the carefully determined viscosity of KNO_3 ²⁰ was found (Table 3).

Uncertainty of the measurements. A complete statistical analysis of error was difficult to obtain from the somewhat complicated expression of eqn. (2) for the sphere. But Table 4 gives the estimated standard deviation of the dif-

Table 4. Estimated uncertainties of measured quantities and corresponding uncertainties for the viscosity.

Variables	Uncertainty, %	Change of value for viscosity, %
Damping, δ	0.5	0.75
Time of swing in nitrogen, T_0	0.04	0.02
Time of swing in liquid, T	0.04	-0.06
Density, ρ	0.3	-0.15
Moment of inertia, I	0.15	0.25
Radius of sphere, R	0.2	-1.0

ferent variables and the resulting changes in viscosity which were calculated from the computer program. The largest uncertainty is introduced in the measurement of the dimensions of the sphere. This is a systematic error and was taken care of as mentioned by a calibration factor. From the scattering and experimental uncertainties we estimated our overall standard deviation to be within 2 %.

Viscosity measurements in pure NaCl, KCl and MgCl₂. In Table 5 the results that were obtained for the pure molten salts are listed. In this temperature range our results show a scatter of about 1 %. In the case of NaCl which has not been cleaned and dried, the results are about 2 % higher than that of anhydrous NaCl. For the density of both NaCl and KCl, we used the data from Van Artsdalen and Yaffe.¹⁸ For MgCl₂ we used the relation given by Grjotheim *et al.*¹⁹

$$d_t = d_{800} \pm (0.38 \times 10^{-3})t$$

$$d_{800} = 1.664$$

From these values we can compute the activation energy for the viscosity, on the assumption that the results can be represented by the well known empirical relation:

$$\eta = A \exp(-E_{\text{vis}}/RT) \quad (46)$$

These results are given in Table 6, in kcal/mole and a comparison is made with literature data. As $\log \eta$ is not a completely linear function of $1/T$ the calculated activation energy will depend on the temperature range chosen.

Table 5. Viscosity in molten NaCl, KCl, and MgCl₂.

Compounds	Exp. No.	Temperature, °C	Viscosity, cP
NaCl without drying	1	812	0.989
	2	854	0.896
	3	858	0.892
	1	884	0.858
NaCl	1	812	0.977
	2	814	0.958
	2	838	0.908
	3	851	0.891
	2	856	0.857
	3	870	0.857
4	885	0.840	
5	902	0.809	
KCl	1	807	0.960
	1	832	0.910
	2	861	0.849
	3	863	0.845
MgCl ₂	1	722	2.127
	2	741	2.015
	2	786	1.856
	3	803	1.759
	3	845	1.642

Table 6. Activation energy for the viscosity in pure salts. Literature values according to Murgulescu and Zuca^{23,24} and Bondarenko.²⁷

Compounds	Temperature range, °C	E_{visc} , kcal/mole This work	E_{visc} , kcal/mole Literature data
NaCl	810–900	4.95	—
	810–970	—	8.69 ²⁴
KCl	810–870	5.52	—
	780–930	—	6.52 ²³
MgCl ₂	730–840	4.76	—
	730–870	—	5.60 ²⁷

Viscosity measurement with cylinder. Viscosities for experiments with the cylinder are summarized in Table 7. The viscosities were calculated from the two different approximations given in the theory and compared with experimental results for the oscillating sphere.

Table 7. Values of viscosities obtained with the oscillating cylinder using eqns. (40) and (41), compared with extrapolated values obtained with the oscillating sphere.

Compounds	Temperature, °C	Viscosity, cP		
		with eqn. (41)	with eqn. (2)	with eqn. (40)
H ₂ O	20.8	1.070	0.995	0.891
KCl	832	0.988	0.906	0.831

DISCUSSION

The successive improvements in our apparatus have enabled us to reduce the scattering of our results to within 1 %. The results obtained for KNO₃ are in good agreement (<1 %) with those reported in the literature,²⁰ so that we can conclude that a satisfactory check of our apparatus has been made.

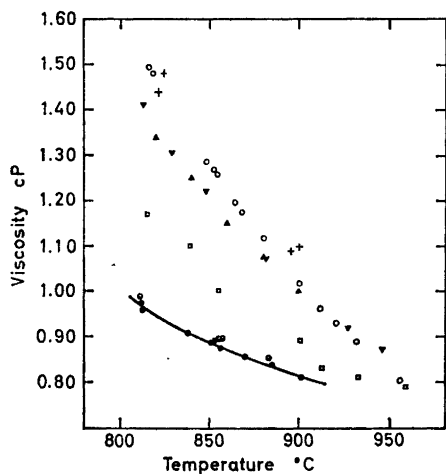


Fig. 5. Viscosity of molten NaCl. Symbols used: + Berenblit;²² ○ Dantuma;²¹ △▽ Murgulescu and Zuca;²⁴ □ Bondarenko;²⁶ ● This work; ◐ Undried salt, this work.

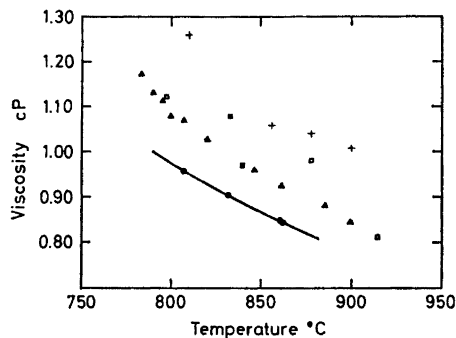


Fig. 6. Viscosity of molten KCl. Symbols used: + Berenblit;²² △ Murgulescu and Zuca;²³ □ Bondarenko;²⁷ ● This work.

The obtained viscosity for NaCl was compared with earlier investigations in Fig. 5. A severe disagreement with earlier investigations was observed both in the actual values and the temperature variation of the viscosity. This discrepancies made us repeat the experiments several times but consistent values were found and the reported values resulted from 7 independent experiments with new loadings of the crucible. The disagreement might pos-

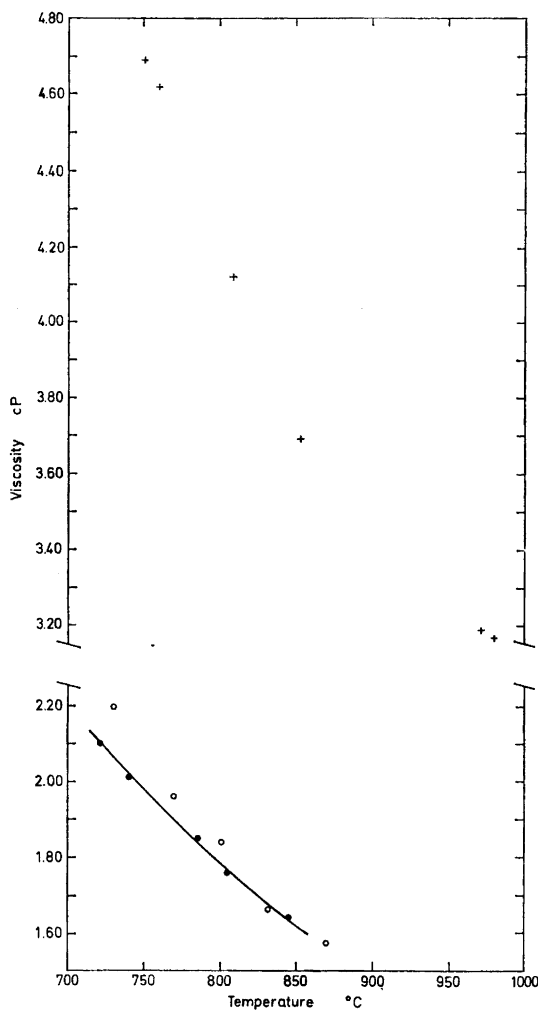


Fig. 7. Viscosity of molten MgCl_2 . Symbols used: ● This work; ○ Bondarenko;²⁷ + Berenblit.²²

sibly have been caused by the earlier workers having the same instability we observed before using an appropriate torsion wire. For instance, Murgulescu and Zuca's²³ results for water and aniline disagree with 15 and 44 % respectively, relative to values given in Landolt-Börnstein's tables,¹⁶ Bondarenko's results²⁶ showed a 10 % scattering.

For KCl (Fig. 6) the variation of viscosity agrees well with previous measurements of Murgulescu and Zuca^{23,24} and Bondarenko²⁷ but our values are consistently about 15 % lower.

For MgCl_2 (Fig. 7) our results agree well with the recent work of Bondarenko²⁷ while an earlier investigation by Berenblit²² gives much higher values.

In Table 7 it is seen that the experimental results for the sphere is about midway between results calculated for cylinder by the two approximations. Referring to Fig. 3, this is what one will expect by physical reasoning. Eqn. (41) takes only consideration to layers projected from the horizontal and vertical sides of the cylinder. But obviously viscous friction will occur in the two rings outside the edges shown as quadrants on the projection on Fig. 2a. Because of neglect of this friction the calculated viscosity will be higher than the real viscosity as shown in Table 4. Using eqn. (40) the viscous drag of layers is larger than in reality, since the layers in the two rings will not move as fast as layers in the same distance which are directly outside the projection of the cylinder. As seen from Table 7 the real physical picture is between the two values, being approximately the mean value of the two approximations. The difference between the two values are approximately 17 % in both cases.

In conclusion it should be pointed out that if the sphere can be utilized it has advantages over the cylinder because it is subject to an easier and a more exact mathematical treatment. Our approximate solutions for the cylinder are, however, so close to the real picture that they can be applied with confidence, introducing an additional coefficient determined by calibration.

Acknowledgement. The work was carried out with a grant from *Norsk Hydro's Forskningsfond ved NTH*. One of us (D.D.) gratefully acknowledges a research fellowship from NATO. We wish to express our gratitude to Mr. Per Osland, Norges Lærerhøgskole for his help in the mathematical derivations and for useful discussions and to Mr. Harry Sagen for technical assistance in the preparation of the anhydrous salts.

REFERENCES

1. MacKenzie, J. D. In Bockris, J. O'M., MacKenzie, J. D. and White, J. L. *Physicochemical Measurements at High Temperatures*, Butterworths, London 1959, p. 313.
2. Umstätter, H. *Einführung in die Viskometrie und Rheometrie*, Springer, Berlin 1952.
3. Blander, M. *Molten Salt Chemistry*, Interscience, Wiley, New York 1964.
4. Sundheim, B. R. *Fused Salts*, McGraw, New York 1965.
5. Thomas, C. W. and Delahay, P. *Advances in Electrochemistry and Electrochemical Engineering*, Interscience, Wiley, New York 1967, Vol. 5.
6. Merrington, A. C. *Viscometry*, Edw. Arnold and Co., London 1949.
7. Bockris, J. O'M. and Lowe, D. C. *J. Sci. Instr.* **30** (1953) 403.
8. Verschaffelt, J. E. *Commun. Phys. Lab. Leiden* **148** b, c, d (1915); **149** b (1916); **151** (1917); **153** (1919).
9. McLachlan, N. W. *Bessel Functions for Engineers*, 2nd Ed., Clarendon Press, Oxford 1955.
10. Motzfeldt, K. In Bockris, J. O'M., MacKenzie, J. D. and White, J. L. *Physicochemical Measurements at High Temperatures*, Butterworths, London 1960, p. 51.
11. Grjotheim, K., Nikolic, R. and Øye, H. A. *Acta Chem. Scand.* **24** (1970) 489.
12. Laitinen, H. A., Ferguson, W. S. and Osteryoung, R. A. *J. Electrochem. Soc.* **104** (1957) 516.
13. Schrier, E. E. *J. Phys. Chem.* **67** (1963) 1259.
14. Bearden, J. E. *Phys. Rev.* **56** (1939) 1023.

15. *Handbook of Chemistry and Physics*, 44th Ed., The Chemical Rubber Co., Ohio 1961.
16. Landolt-Börnstein, *Zahlenwerte und Funktionen*, 6 Aufl. IV Band, 1. Teil, Springer, Berlin 1955.
17. Brillant, S. *Thesis*, Strasbourg University 1967.
18. Van Artsdalen, E. R. and Yaffe, D. S. *J. Phys. Chem.* **59** (1955) 118.
19. Grjothheim, K., Holm, J. L., Lillebuen, B. and Øye, H. A. Submitted to *Trans. Faraday Soc.*
20. Kleinschmit, P. *Diss. Tech. Hochschule Hannover* 1968.
21. Dantuma, R. S. *Z. allgem. anorg. Chem.* **175** (1928) 1.
22. Berenblit, V. M. Cited in Strelets, Kh. L., Jaiz, A. J. and Gulpantizki, B. *Metallurgie des Magnesium*, Verlag Technik, Berlin 1953, p. 199.
23. Murgulescu, I. G. and Zuca, S. *Z. physik. Chem. (Leipzig)* **218** (1961) 379.
24. Murgulescu, I. G. and Zuca, S. *Z. physik. Chem. (Leipzig)* **222** (1963) 300.
25. Murgulescu, I. G. and Zuca, S. *Revue Roumaine de Chimie* **10** (1965) 123.
26. Bondarenko, N. V. and Strelets, Kh. L. *J. Appl. Chem. USSR* **38** (1965) 1273.
27. Bondarenko, N. V. *J. Appl. Chem. USSR* **39** (1966) 2684.

Received July 5, 1969.